

Fabrication, thermal, and dielectric properties of self-passivated Al/epoxy nanocomposites

Wenying Zhou · Demei Yu

Received: 4 June 2013 / Accepted: 16 July 2013 / Published online: 25 July 2013
© Springer Science+Business Media New York 2013

Abstract The current paper reports the effects of an epoxide-functionalized, silane surface-treated, self-passivated aluminum (Al) nanoparticles on the glass transition, morphology, thermal conductivity, dielectric properties of an epoxy composite. The surface modification of the Al nanoparticles improved the dispersion of the filler, as well as the glass transition temperature, thermal conductivity, and dielectric properties of the epoxy composites. The epoxy/Al nanocomposites showed a dielectric constant transition concentration. The dielectric constant and dissipation factor increased when the Al particle loading exceeded the critical content but gradually decreased with the frequency. The epoxy nanocomposites containing 15 % by weight Al nanoparticles have a high thermal conductivity and a high dielectric constant but a low dissipation factor. The enhancements in the thermal and dielectric properties of the epoxy nanocomposites show potential for future engineering applications.

Introduction

Polymer-based nanocomposites which are binary combination of continuous polymeric matrix and nanosized particles have attracted considerable attentions and have been

widely explored owing to their particular mechanical, magnetic, electrical, and thermal properties [1–3], meanwhile, their advantages, such as flexibility, easy processing, and tunable properties, make them most preferably applicable in electronic materials [4, 5].

Nowadays, embedded capacitors are specially printed portions of printed circuit board (PCB) laminates that perform the charge-storing function but do not require space on the PCB surface. Embedded capacitors are widely used for various functions, such as decoupling, by-passing, filtering, termination, and energy storage [6], and they are also capable of enhancing the electrical performance and reducing the size and cost of an electronic system. One major technical challenge to implement this emerging embedded-capacitor technology is the development of appropriate dielectric materials with good electric and mechanical properties, as current PCBs manufacturing methodologies cannot apply traditional ceramic dielectrics [7]. Functional polymer nanocomposites with high dielectric permittivity are promising candidates as dielectrics in the embedded capacitors-component technology due to the flexibility and good compatibility with organic PCBs. The various metallic powders (Ag, Cu, Al) [6–9], carbon materials (carbon black, carbon nanotube, carbon fiber and graphene) [10–15] and ceramic particles (BaTiO₃, PMN-PT) [16–18] have been employed as fillers to improve the polymer's conductivity and dielectric properties. Until now, extensive attention was focused on the preparation of a polymeric nanocomposite with high dielectric constant, low dielectric loss for the applications in embedded capacitors and PCB substrates; however, the thermal conductivity of the composites has been rarely investigated and reported. The increasingly miniaturized embedded component subsequently leads to an escalation of power dissipation as well as an increase in heat flux when the

W. Zhou (✉)
College of Chemistry and Chemical Engineering, Xi'an
University of Science & Technology, Xi'an 710054,
People's Republic of China
e-mail: wyzhou2004@163.com

W. Zhou · D. Yu
State Key Laboratory of Electrical Insulation & Power
Equipments, Xi'an Jiaotong University, Xi'an 710049,
People's Republic of China

electronic device is in work under high frequency [19–21]. As such, the heat dissipation problem poses a potential threat to the lifespan of high-performance electronic devices [22, 23]. Thus, it is crucial that the heat generated in the embedded capacitors-component should be dissipated as quickly as possible, maintaining the device's desired operating temperature [24–26]. Therefore, the development of a polymer composite with high thermal conductivity and dielectric permittivity but low dielectric loss is very important because high thermal conductivity facilitates to prolonging the lifespan of polymeric embedded capacitors-component [22].

The preparation of percolative dielectrics with a threshold composition is difficult because of the abrupt variations in the dielectric constant and loss near the threshold. The high dielectric constant composite requires a uniform dispersion and precise control of the loading filler because of its percolative nature [7]. Surface self-passivated aluminum (Al)/polymer composites have the combined advantages of a percolative composite and a ceramic/polymer system. The core is metallic Al, which confers a high dielectric constant to the percolative composite system, and the nanoscale shell is an insulating Al oxide, which confers a low dielectric loss comparable to that of a neat epoxy resin [2, 6]. Xu [6] prepared epoxy nanocomposites containing up to 40 wt% Al particles (100 nm), with a maximum dielectric constant of 80 and a dissipation factor of 0.02. However, the thermal conductivity of this epoxy nanocomposite was not investigated.

The current paper aims to examine the effect of Al nanoparticles at low loading levels on the thermal and dielectric properties of epoxy. A surface self-passivated Al nanoparticle (80 nm) was used as the filler, and an epoxy resin was used as the matrix resin because of its good mechanical properties, low water uptake, low coefficient of thermal expansion, and easy processing. In this work, a conventional mixing method was used to prepare the samples without using any inert organic solvents. To obtain a good dispersion of Al nanoparticles in the epoxy, an epoxy-functionalized silane coupling agent was applied to functionalize the Al nanoparticle surfaces, thereby improving the interfacial adherence and stability of the Al nanoparticles and enhancing the dielectric and thermal conductivity of the Al/epoxy nanocomposites.

Experimental

Materials

The polymer matrix used was a diglycidyl ether of a bisphenol A-type epoxy resin (D.E.R-331, Dow Chem. Corp., USA) with a 0.52 to 0.54 epoxy value. A flexible

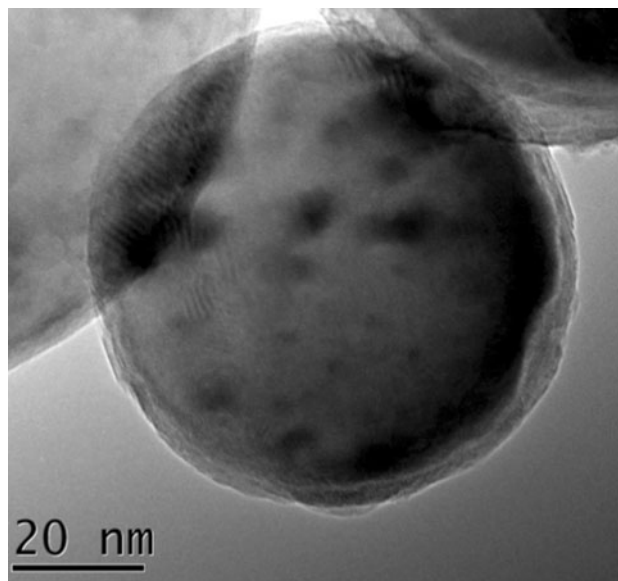


Fig. 1 High resolution TEM micrograph of an 80 nm aluminum particle

epoxy resin (long-chain polyglycol diepoxide liquid resin, D.E.R-732, Dow Chem. Corp., USA) was used as a reactive toughening agent to overcome the brittleness of the matrix. The curing agent was methyl hexahydrophthalic anhydride (MeHHPA, Shanghai Shengyuan Co., China), and the cure accelerator was 2,4,6-tri(dimethylamino-methyl) phenol (DMP-30, Shanghai Haitai Co., China). Nano Al powder (80 nm) was purchased from Xuzhou Hongwu Nano Co. (Jiangsu, China). (3-Glycidyloxypropyl)-trimethoxysilane (Nanjing Shuguang Chemical Co.) was used as a coupling agent. Other chemical reagents were all commercially available. The high-resolution transmission electron microscopy (TEM) image of an 80 nm Al particle is shown in Fig. 1.

Sample preparation

Surface modification of Al nanoparticles

Nano Al particles were treated with silane using a method similar to that reported in the literature [22]. A 95 % ethanol/5 % water solution was prepared and its pH was adjusted to 4–5 using dilute hydrochloric acid. Silane was added to this solution with continuous stirring and kept for 20 min for hydrolysis and silanol formation. Meanwhile, Nano Al particles were dispersed in ethanol solution via bath ultrasonication for 50 min for deagglomeration. The two solutions were subsequently mixed together, and the mixture was refluxed at 80–90 °C for 6 h, and 120 °C for 2 h to complete the wetting of the nano Al particles with silanol. The mixture was then cooled to room temperature for 3 h, and then rinsed with ethanol at least three times.

The final mixture was centrifuged, and the Al particles were collected and dried at 120 °C for 12 h.

Al/epoxy composite preparation

The low-viscosity toughening agent and the liquid anhydride MeHHPA were used to reduce the viscosity of the Al/epoxy system. The maximum Al content was set at 15 wt% because a higher filler concentration can result in the loss of natural flow property of the mixed system.

The mass ratio of the epoxy D.E.R-331, the D.E.R-732, the MeHHPA, and the DMP-30 was kept at 70:30:85:0.5. The epoxy resin D.E.R-331 was blended with the flexible epoxy D.E.R-732, MeHHPA, Al nanoparticles, and DMP-30, respectively. All the blended mixture was then ultrasonicated for 30 min at 40 °C and stirred vigorously for 1 h; afterward, the obtained homogeneous mixture was degassed for 20 min in a vacuum to remove the bubbles. The liquid mixture free of solvent was then poured into a clean glass plate mold kept at 80 °C and cured in an oven at 110 °C for 1 h and 150 °C for 5 h. Finally, the cured sample was left to slowly cool down to room temperature. This procedure was used to prepare solvent-free, epoxy-based composites with Al nanoparticle concentrations ranging from 0 to 15 wt%.

Characterization

The surface chemistry of the Al nanoparticles was determined using a Fourier transform infrared (FT-IR) spectrometer (Perkin-Elmer, Paragon 1000). The Al particles were first dried in an oven at 110 °C for 3 h, then Al particles were mixed with KBr and the mixture was compressed into pellets. The spectrum in the 4000–400 cm^{-1} range was recorded.

Sample weight loss upon heating was measured using a thermogravimetric analyzer (TGA, SDTA851, Swiss). The measurements were performed from 25 to 600 °C at a heating rate of 15 °C min^{-1} under a nitrogen atmosphere.

The glass transition temperatures of the nanocomposites were measured using a differential scanning calorimeter (DSC, Perkin-Elmer Pyris 6). The samples were heated from 20 to 200 °C at a heating rate of 10 °C min^{-1} . All measurements were conducted in a nitrogen atmosphere.

A scanning electron microscope (SEM, JEM-7000F, Japan) and TEM (JEM-2100, Japan) were used to observe the dispersion of the Al nanoparticles in the composite samples. For the SEM observation, the samples were broken and the fractured surface was sputtered with a thin layer of gold to prevent charge accumulation.

A hot disk thermal analyzer (Hot Disk AB, Uppsala, Sweden) was used to measure the thermal conductivity of

the samples using the transient plane source (TPS) method, which is based on a transient technique. A disk-shaped TPS sensor 7 mm in diameter and 0.07 mm thick was placed between two circular sample pieces 20 mm in diameter and ~1 mm thick.

The dielectric measurement was performed at room temperature using a broadband dielectric spectrometer (Novocontrol Technology Company, Germany) with an Alpha-A high-performance frequency analyzer to investigate the frequency-dependence of the dielectric property. Before the dielectric characterization, electrodes were painted on the sample using silver paste. The specimens for the dielectric measurement were made into circular discs ~1 mm thick and 20 mm in diameter.

Results and discussion

FT-IR characterization

The surface modification of Al nanoparticles was determined via FT-IR measurements. Figure 2 shows the FT-IR spectra of both the untreated and silane coupling agent surface-treated Al nanoparticles. An obvious wide absorption peak at about 3200–3700 cm^{-1} can be observed in Fig. 2a, which is characteristic of the stretching vibration of –OH groups on the surface of untreated Al nanoparticles; whereas, the absorption peak disappears for the silane coupler treated Al nanoparticles as seen in Fig. 2b. Because the surfaces of Al nanoparticles were enriched in hydroxyl groups, clear stretching vibration of –OH groups for untreated Al nanoparticles was observed; the active chemical groups (hydroxyl, –OH) of the coupling agent were assumed to be chemically grafted onto the surface of

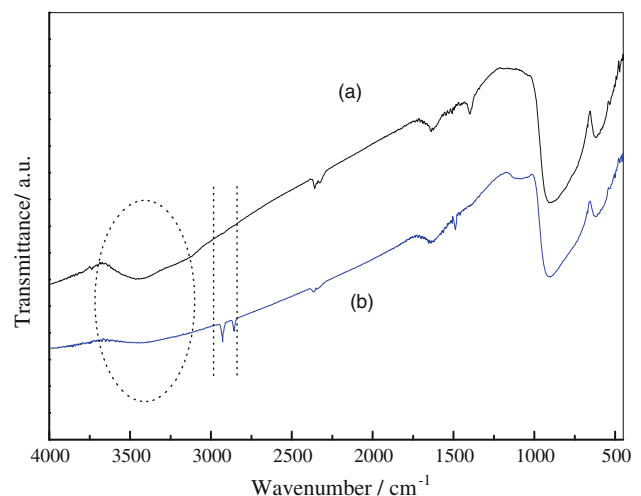


Fig. 2 FT-IR spectra of untreated (a) and silane treated (b) nano Al particles

the Al nanoparticles after surface treatment [27]. Thus, the surfaces of Al nanoparticles were covered by a layer of coupling agent, and the absorption peak of $-OH$ groups was no longer observed. Moreover, the new adsorptions at about 2853 and 1924 cm^{-1} are the characteristics for stretching vibration of the $C-H$ bond of the silane, where, the signal at 1492 cm^{-1} is assigned to bending vibration of the $-CH_2-$ group of the silane coupler compared with the without surface modification of Al nanoparticles. Based on above results, we can conclude that the active chemical groups of the coupling agent were chemically grafted onto the surface of Al nanoparticles.

TGA characterization

Figure 3 shows the TGA curves of the surface-treated and untreated Al nanoparticles. Two stages of weight loss can be observed for the two nanoparticle types. At a low temperature range ($<180\text{ }^\circ\text{C}$), the weight loss is ascribed to the removal of water molecules physically absorbed onto the surface of the nanoparticles. At the $50\text{--}600\text{ }^\circ\text{C}$ temperature range, the weight loss may be due to the condensation of the silanol groups and the decomposition of the grafted silane molecules. The weight loss of the surface-treated nanoparticles was clearly higher than that of the untreated nanoparticles, indicating that the silane molecules were successfully grafted onto the surface of the Al nanoparticles [28].

Glass transition temperatures

Epoxy resins, which are chemically hardenable plastics (or chemosets), soften at the glass transition peak temperature (T_g or softening temperature) and deform under a load. Afterward, many physical properties exhibit remarkable

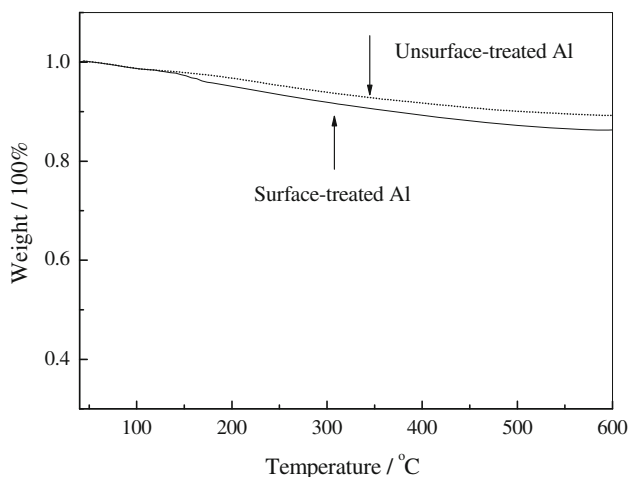


Fig. 3 TGA curves of surface-treated and unsurface-treated Al nanoparticles

changes [28]. Polymers having excellent insulating properties at temperatures below T_g may exhibit semiconducting characteristics at temperatures above T_g . Therefore, T_g is considered as the most important material property of epoxy resins.

Figure 4 shows the T_g of the Al/epoxy nanocomposites obtained from the DSC measurements. T_g increased with increasing filler loading (up to 8 wt%); at 8 wt%, T_g started to decrease with increasing Al nanoparticle concentration. The T_g values of the nanocomposites were slightly higher than that of the pure epoxy before the loading levels reached 15 wt%. Glass transition in polymers is a complex phenomenon that is affected by a number of factors, including the free volume, molecular chain segments mobility, molecular weight, and crosslink density [29]. In the present study, the T_g of epoxy nanocomposites may be affected by the free volume, the interaction between the nanoparticles and the matrix, and the crosslink density. The grafting of silane onto the Al nanoparticles enhanced the interaction between the matrix and the fillers, resulting in a decrease in the free spaces at the interface between the epoxy molecules and fillers, and a restriction of epoxy chain segments rotation or movement. Thus, surface-treated nanoparticles reinforced the molecular chains of the epoxy resin and compensated for some defects in the cured networks as compared to the neat epoxy, resulting in a slight decrease in the motion ability of the epoxy chain segments. Therefore, the T_g values of the surface-treated nanoparticles/epoxy are higher than that of the neat epoxy [28]. When the mass fraction of the Al nanoparticles exceeded 8 wt%, the T_g of the epoxy nanocomposites started to decrease above 8 wt% Al. The reason can be ascribed to the followings: (1) the effective surface area of the nanofillers began to decrease a little because of the agglomeration of the Al nanoparticles; (2) the more Al nanoparticles may reduce the crosslink density of epoxy

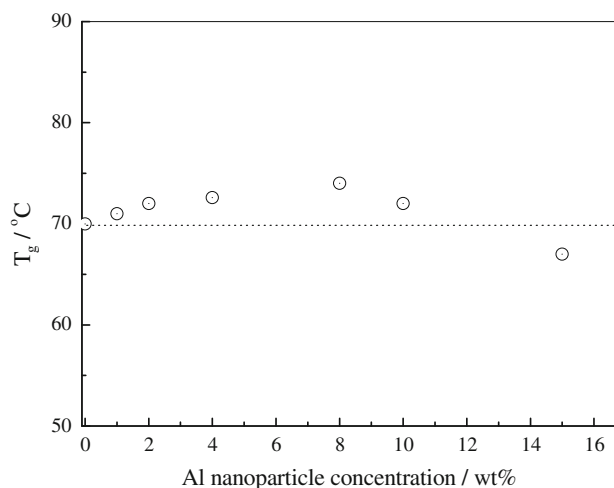


Fig. 4 Glass transition peak temperature (T_g) of epoxy/Al nanocomposites

network because the existence of Al nanoparticles disturbs the curing process of epoxy and hardener, thus improving and facilitating the large-scale mobility of the epoxy chain segments. So, the lower T_g of the epoxy with 15 wt% Al nanoparticles was observed. The DSC results indicate that the incorporation of Al particles into the epoxy composites changed the mobility of the epoxy molecules chain segments, resulting in the difference in the T_g of the nanocomposites.

Morphology and dispersion

Inorganic nanoparticles can spontaneously aggregate because of their large surface area and high surface energy. One possible technique to overcome this problem is to modify the nanoparticle surface, which can be achieved using surfactants and polymers that are physically adsorbed on particles only via electrostatic attraction or van der Waals forces. In the current study, the (3-glycidyloxypropyl)-trimethoxysilane coupler was used as an interlayer to form a chemical linkage between the Al nanoparticles and the epoxy matrix, thereby improving the compatibility of the separated phases.

Figure 5 shows the microstructure of the fractured surfaces of the neat epoxy and the surface-treated Al/epoxy nanocomposites. The fractured paths with river-like line patterns can be observed in Fig. 5a, indicating brittle fractures on the cured neat epoxy surface. Figure 5b and c show that most of the nanoparticles are embedded in the epoxy matrix, with no clear evidence of Al particle-matrix

debonding, suggesting a relatively strong interfacial bonding and good compatibility between the Al nanoparticles and the epoxy [28]; only a very small amount of nanoparticles were exposed outside. The Al nanoparticles act as stress concentrators to absorb some of the impact energy and initiate a higher degree of plastic deformation. This deformation promotes stress transfer between the nanoparticles and the epoxy matrix, resulting in rough fractured surfaces. Unlike the cured pure epoxy, the Al/epoxy composites show a rough fracture surface due to the matrix shear yielding or local polymer deformation.

The nanocomposites prepared in the current study showed no large obvious Al nanoparticle conglomerations and agglomerations, indicating a uniform dispersion of the nanoparticles in the epoxy matrix. The reason is mainly attributed to the substitution of hydroxyl groups on the surface of Al with the 3-glycidyloxypropylsilyloxy groups of the silane coupling agent grafted on the surface of Al. The coupling agent gave a dual positive effect by lowering the interfacial tension between the separated phases and preventing the coalescence of the nanoparticles during processing [30, 31]. The active chemical groups of the coupling agent are assumed to be chemically grafted onto the surface of the Al nanoparticles, which was confirmed by the FT-IR result. A schematic diagram showing the reaction mechanism of the silane coupler with the $-OH$ groups on the surface of an Al particle is shown in Fig. 6. The methoxy groups of the silane coupler were first hydrolyzed by water to form three silanol groups; then,

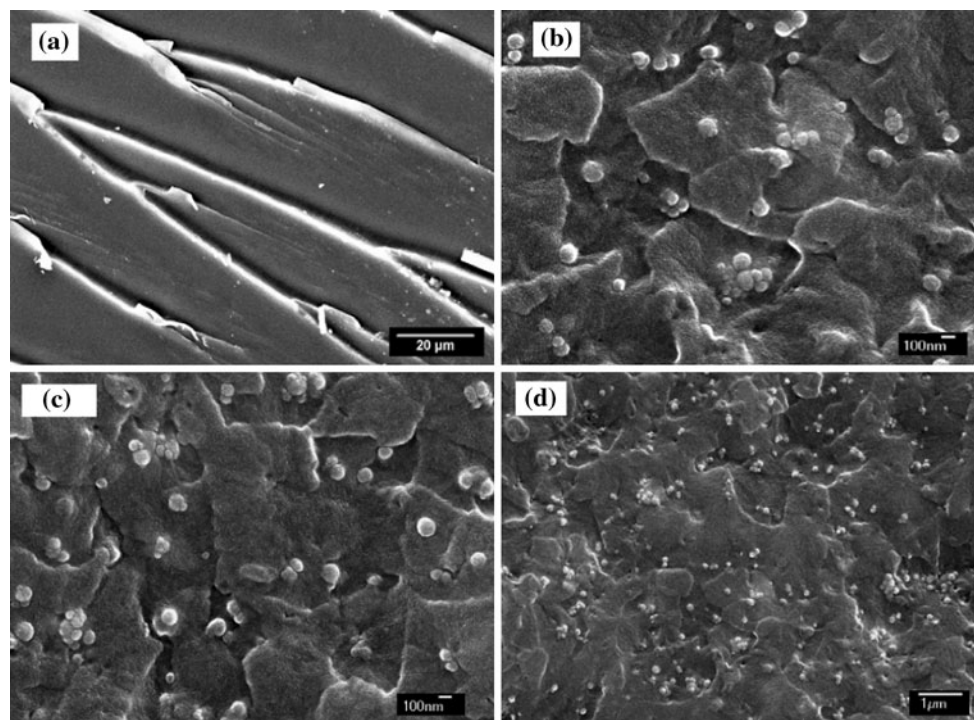
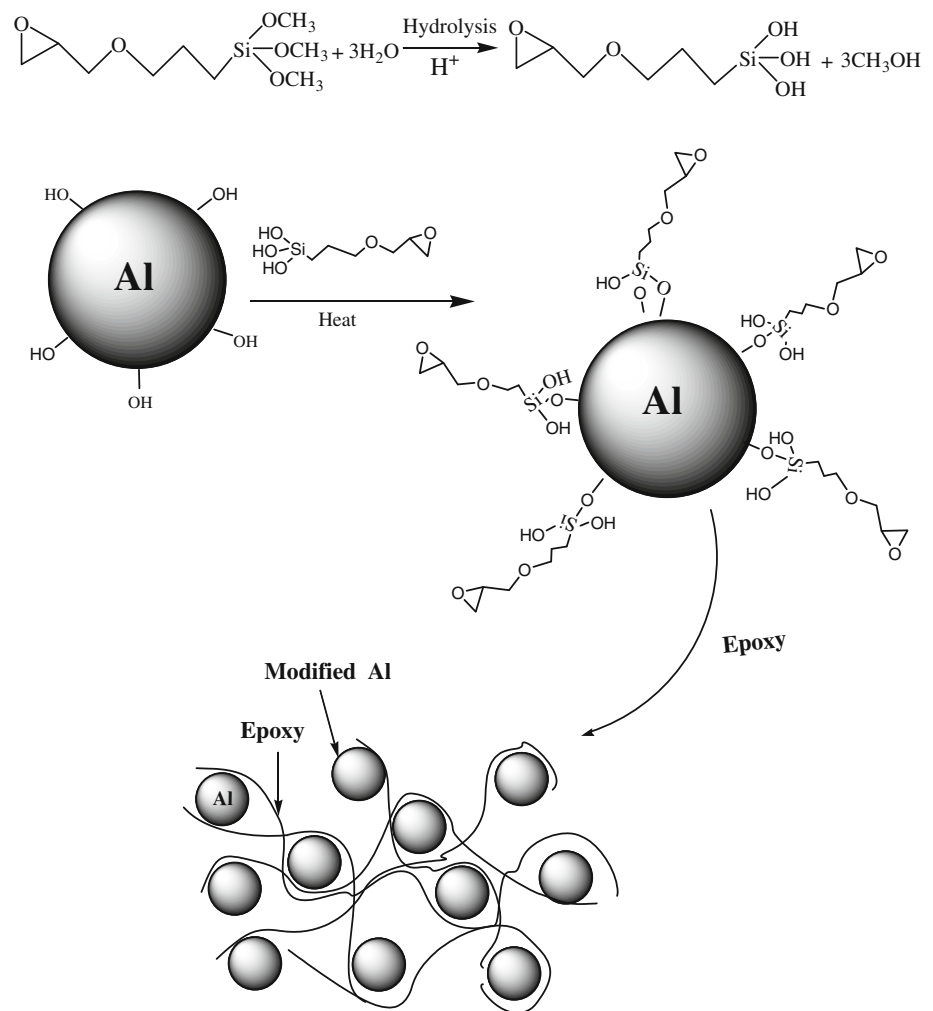


Fig. 5 SEM images of epoxy/Al nanocomposites at different filler loading: **a** 0 wt%, **b** 6 wt%, **c**, **d** 10 wt%

Fig. 6 Schematic showing the reactions of (3-glycidyloxypropyl)-trimethoxysilane coupling agent with Al nanoparticle surface, and the compatibility between the surface-modified Al nanoparticles and epoxy matrix



these silanol groups were condensed with the hydroxyl groups on the alumina shell of the Al to form the Si–O–Al bond via acid-catalyzed reactions.

The silane coupling agent treated Al nanoparticles show good compatibility with epoxy matrix because the epoxy groups grafted on the surface of Al filler either chemically react with the anhydride curing agent, or interact with the epoxy long chains, thereby providing strong interfacial interaction between the two components, which reduces the number of air voids ($k_{\text{air}} = 0.0024 \text{ W mK}^{-1}$) and defects at the interfacial phase. This action can enhance the thermal conductivity of the composites because of the reduced interfacial thermal contact resistance and other physical properties as compared to untreated ones.

Thermal conductivity

The thermal conductivity values of the epoxy and epoxy/Al nanocomposites are shown in Fig. 7. The thermal

conductivity of the epoxy matrix gradually increased with the increase in Al nanoparticle content because of the high thermal conductivity of the filler. At 10 wt% (3.95 vol%) and 15 wt% (6.34 vol%) Al nanoparticle loading, the thermal conductivity of the epoxy increased by 17 and 43 %, respectively. These enhancements in thermal conduction confer potential applications for the epoxy/Al nanocomposites.

Several models can be used to compare the theoretical predictions for the epoxy/Al nanocomposites with the current experimental results. These theoretical and empirical models were proposed to clarify the phenomenon behind the thermal conductivity of composites containing two components and involving several factors. Dispersion, nanoparticle size and shape and their interaction, interfacial resistance, and other factors were considered when the models were designed [10]. The Maxwell–Eucken, Series, Zhou, and Bruggeman models were used to evaluate the thermal conductivity of the epoxy/Al nanocomposites.

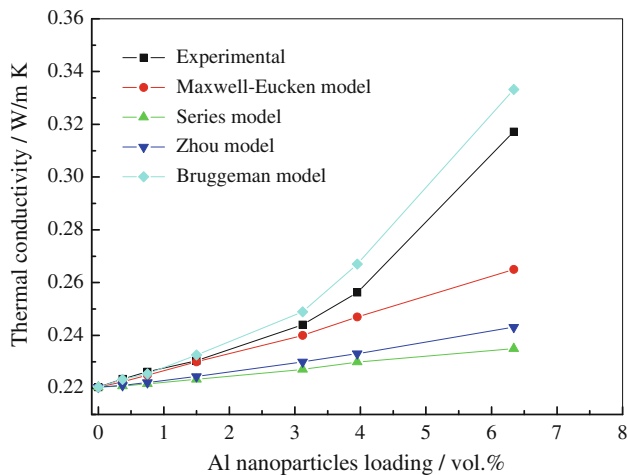


Fig. 7 The experimentally determined thermal conductivity values of the composites and the values predicted from theoretical models

Maxwell–Eucken model:

$$k_c = k_m \frac{2k_m + k_f + 2V_f(k_f - k_m)}{2k_m + k_f - V_f(k_f - k_m)} \quad (1)$$

Series model: $\frac{1}{k_c} = \frac{1 - V_f}{k_m} + \frac{V_f}{k_f}$ (2)

Zhou model: $k_c = k_m \left[1 + \frac{V_f(k_f - k_m)}{k_f - V_f^{1/3}(k_f - k_m)} \right]$ (3)

Bruggeman model: $1 - V_f = \frac{k_f - k_c}{k_f - k_m} \left(\frac{k_m}{k_c} \right)^{1/3}$ (4)

where k_c , k_m , and k_f are the thermal conductivity of composites, polymer and filler, respectively; V_f is the volume fraction of filler.

In Fig. 7, the thermal conductivity values obtained from the experimental study were compared with those of several models. The Maxwell, Series, and Zhou models evidently underestimated the thermal conductivity of the composites, whereas the Bruggeman model gave acceptable predictions. Figure 7 suggests that the calculated values were either slightly higher or lower than the experimental results, proving that these models are unsuitable for the current system and that other parameters such as the interfacial resistance, size and shape of the filler, and so on need to be considered [10].

Dielectric properties

The dielectric constant demonstrates the ability of a material to store electric potential energy under an alternating electric field. Figure 8 shows the frequency-dependence of the dielectric constant and the dissipation factor of the epoxy/Al nanocomposites with different Al loading levels measured at room temperature, these phenomena are

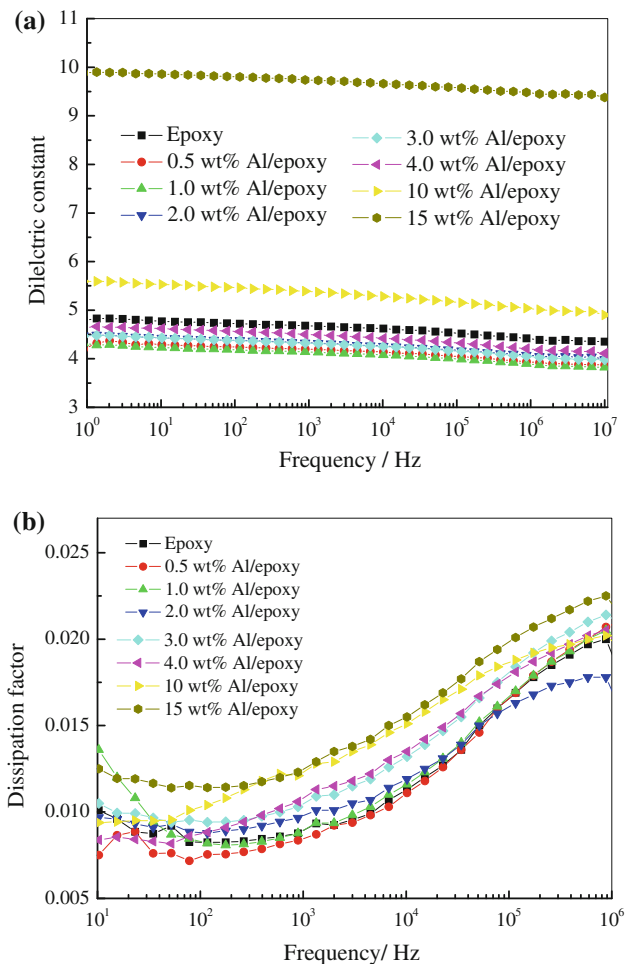


Fig. 8 Dielectric properties versus frequency for neat epoxy and epoxy/Al composites: **a** Dielectric constant, **b** dissipation factor

characteristic of polar polymers. Figure 8a shows that the effective dielectric constant of the neat epoxy and the epoxy/Al nanocomposites exhibited a very low frequency-dependence, which slightly decreased with the frequency. The addition of Al nanoparticles initially caused a decrease in the overall level of the dielectric constant compared with the neat epoxy. However, further loading of Al up to above 4 wt% resulted in an increase in the dielectric constant to a level higher than that of the neat epoxy. A critical concentration of approximately above 4 wt% was found to exist in the epoxy/Al nanocomposites. Below or above this level, the dielectric constant values become lower or higher than those of the neat epoxy under various applied sweep frequencies, respectively. The dielectric constant often increases when the polymers are filled with inorganic or conductive fillers because of the inherently higher dielectric constant of the fillers compared with those of the polymer matrix and the interfacial polarization. However, lower dielectric constant values for the composites at low filler loading were observed in some polymer nanocomposites

such as epoxy/TiO₂, epoxy/ZnO, epoxy/AlN, and polypropylene/carbon nanofiber [10, 28, 32]. In these nanocomposites, the fillers possess a significantly higher dielectric constant compared with that of the base polymer, and interfacial polarization occurs. Some researchers believe that the increase in free volume and the number of voids can cause a reduction in the dielectric constant, especially in the untreated nanoparticle/polymer composites [33, 34], because these nanoparticles can introduce more free volume and voids resulting from the greater steric volume and agglomeration of the nanoparticles. A correlation between a large free volume and high number of voids with a low dielectric constant has been previously observed in several polymers [34]. Other scholars proposed that both an improvement in the conductivity of the composite and a variant degree of crystallinity or cure of the polymer matrix, which affects the dipole polarization of the groups and chain segments within the matrix, may explain the reduction in the dielectric constant of the composites at low filler loading [10]. Thus, the crystalline characteristic of the polymer matrix is also an important factor that determines the dielectric properties of the composites.

From Fig. 5, we can observe that no large obvious Al nanoparticle conglomerations and agglomerations exist, indicating improved interfacial bonding strength between the filler and matrix, and a uniform dispersion of the nanoparticles in the matrix, therefore, it is impossible that the increase in free volume and the number of voids cause a reduction in the dielectric constant for the treated Al nanoparticle/polymer composites. The restriction of macromolecular chain segments movement by nanoparticles in the current study can be considered a major reason for the reduction in the dielectric constant [33, 35] at low filler loading. For polar polymers such as epoxy, the mobility of the dipolar groups contributes to the dielectric constant of the composites [32]. Two competitive factors may be affecting the dielectric constant of the epoxy/Al nanocomposites, depending on the combination of the interfacial polarization and the interactions between the epoxy and the nanoparticles. Below the critical filler concentration, the incorporation of Al results in little mobility of the polymer chain segment because the stronger interaction at the interfacial phase exhibits an advantage over the interfacial polarization, resulting in a reduction in the dielectric constant. On the other hand, the incorporation of Al nanoparticles with a concentration above the critical value gave the opposite results. A dielectric constant higher than that of neat epoxy can be ascribed to the increase in the number of polarizable groups with the addition of Al nanoparticles because of lower curing degree of cured epoxy network resulting from the more nanoparticles, which can enhance the polarization under an electrical field.

The variation in the dielectric constant with the frequency indicates the occurrence of an interfacial polarization in the epoxy composites. The very slight decrease in the dielectric constant with increasing frequency is believed to be caused by the slow dielectric relaxation of the matrix resin and the interface of the composites [10]. At low frequencies, all dipole groups in the polymer molecular chains can orient themselves, resulting in a higher dielectric constant. By contrast, as the frequency further increases, the polarization fails to stabilize completely and the values of the dielectric constant decrease.

The dielectric dissipation factors of neat epoxy and the epoxy/Al nanocomposites under various applied sweep frequencies are plotted in Fig. 8b. The dissipation factors of the samples initially exhibited little decreases with increasing frequency, followed by an increase to 10⁶ Hz.

The initial increase in dissipation factor at low frequency primarily can be ascribed to the conductivity because the dissipation factor depends mainly on the content of ionic contaminants within the polymer matrix (which are the charge carriers) at low frequencies; in addition, the dipole polarization loss is another reason for the loss increases [36] because of the self-orientation of dipoles in the direction of the alternating field with decreasing frequency. Further increasing the frequency leads to a decrease in dipole polarization effects and the dissipation factor. However, the dielectric loss tangent tends to increase when the frequency is above 1.0 kHz; a peak of the dielectric loss tangent of the composites appeared at approximately 10⁶ Hz. This result is attributed to an obvious relaxation loss caused mainly by segmental movements of the epoxy matrix [2] at high frequencies. So, there are two different mechanisms of the losses.

The dissipation factor of the composites slightly increased with Al nanoparticle loading. With increased Al nanoparticle content, the charge carriers within epoxy contributing to the dissipation factor increased and caused an increase in the dielectric loss of the composites; while, at low Al nanocomposites loading level of 0.5 wt%, Al could inhibit the movement of the charge carriers or cause a reduction in the electric conductivity, thereby leading to a lower dissipation factor values compared with those of neat epoxy. It was reported [28] that two competitive factors may be affecting the dissipation factor of the epoxy/Al composites depending on the hindrance in the charge transport and the incorporation of the charge. As the Al loading further increased, the effect of charge carrier immobility on the reduction in the electric conductivity was negligible compared to the effect of the content of ionic contaminants introduced by Al loading. Therefore, the dissipation factor increased with Al loading [28, 34]. However, at a high loading of 15 wt% of Al, the nanocomposites still exhibited a low dissipation factor mainly

because of the insulating nanoscale Al oxide shell of the Al nanoparticle (as seen in Fig. 1) acting as an interlayer between the Al cores.

In the 1–10⁶ Hz frequency range, the composites with 15 wt% Al exhibited a high and relatively stable dielectric constant, and in the 10–10⁶ Hz frequency range the dissipation factor of the composites with 15 wt% Al was at a low level (generally <0.024), which satisfy the requirement for a high dielectric permittivity but low loss value in practical engineering applications.

Conclusions

The effects of Al nanoparticles surface-treated with an epoxide-functionalized silane coupler on the glass transition, morphology, thermal conductivity, and dielectric properties of epoxy composites were investigated in terms of Al loading.

The FT-IR and TGA results suggest that the active chemical groups of the coupling agent could be chemically grafted onto the surface of Al nanoparticles, resulting in better nanoparticle dispersion in the epoxy resin. The enhanced interfacial interaction between the Al nanoparticles and epoxy induced by surface chemical modification could lead to an increase in the T_g , and improved thermal conductivity of the epoxy nanocomposites.

The epoxy/Al nanocomposites showed a dielectric constant transition concentration. Above this transition concentration, the dielectric constant was larger than that of the neat epoxy, whereas below this level, the opposite results were observed. A dissipation factor transition concentration was also found for the epoxy/Al nanocomposites at very low Al nanoparticle loading.

The epoxy nanocomposites containing 15 wt% Al have a thermal conductivity of 0.32 W mK⁻¹, a dielectric permittivity of 10, a very low dissipation factor of 0.024 resulted from the insulating nanoscale Al oxide shell of the Al nanoparticle acting as an interlayer between the Al cores. The enhancements in the thermal and dielectric properties of the nanocomposites show potential in future engineering applications.

Acknowledgements The authors gratefully acknowledge the financial supports from China Postdoctoral Science Foundation

(No. 200801434), the Foundation for Key Program of Ministry of Education, China (212175), and National Science Foundation of China (No. 51073180).

References

1. Wang FJ, Li W, Xue MS et al (2011) *Composites B* 42:87
2. Zhou WY, Yu DM (2010) *J Appl Polym Sci* 118:3156
3. Dang ZM, Yu YF, Xu HP (2008) *Compos Sci Technol* 68:68
4. Popielarz R, Chiang CK (2007) *Mater Sci Eng B* 139:48
5. Huang XY, Jiang PK, Kim CU (2008) *Compos Sci Technol* 68:2134
6. Xu JW, Won CP (2007) *Compos A* 38:13
7. Qi L, Lee Burtrand L, Chen S (2005) *Adv Mater* 17:1777
8. Shen Y, Lin YH, Nan CW (2007) *Adv Mater* 19:1418
9. Prakash SB, Varma KBR (2007) *Compos Sci Technol* 67:2363
10. Sui G, Jana S, Zhong WH (2008) *Acta Mater* 56:2381
11. Yang SY, Lin WN, Huang YL et al (2011) *Carbon* 49:793
12. Cui W, Du FP, Zhao JC et al (2011) *Carbon* 49:495
13. Logakis E, Pollatos E, Pandis C et al (2010) *Compos Sci Technol* 70:328
14. Deng HY, Wang XY, Chen QY et al (2011) *Mater Sci Eng A* 528:759
15. Kim JB, Yi JW, Nam E (2011) *Thin Solid Films* 519:5050
16. Kim DW, Lee DH, Kim BK et al (2006) *Macromol Rapid Commun* 27:1821
17. Kim P, Jones SC, Horchkiss PJ et al (2007) *Adv Mater* 19:1001
18. Arbatti M, Shab XB, Cheng ZY (2007) *Adv Mater* 19:1369
19. Zhou WY, Qi SH, An QL (2007) *Mater Res Bull* 42:1863
20. James RG, Yvonne YV, Steven B (2003) *Carbon* 41:2187
21. Giuseppe P, Ikuko K (2000) *J Eur Ceram Soc* 20:1197
22. Zhou WY, Qi SH, Tu CC (2007) *J Appl Polym Sci* 104:2478
23. Ruth R, Donaldson KY, Hasselman DPH (1992) *J Am Ceram Soc* 75:2887
24. Kumlutas D, Ismail H, Tavman M (2003) *Compos Sci Technol* 63:113
25. Samuels RJ, Mathis NE (2001) *Electron J Packag* 23:272
26. Ishida H, Rimdusit S (1998) *Thermochim Acta* 320:177
27. Zhou WY (2011) *J Mater Sci* 45:3883. doi:10.1007/s10853-011-5309-y
28. Peng WY, Huang XY, Yu JH (2010) *Compos A* 41:1201
29. White SR, Mather PT, Smith MJ (2002) *Polym Eng Sci* 42:51
30. Huang XY, Jiang PK, Yin Y (2009) *Appl Phys Lett* 95:905
31. Huang XY, Kim CU, Jiang PK et al (2009) *J Appl Phys* 105:014105
32. Singha S, Thomas MJ (2008) *IEEE Trans Dielectr Insulation* 15:12
33. Tanaka T, Kozako M, Fuse N (2005) *IEEE Trans Dielectr Insulation* 12:669
34. Tanaka T (2005) *IEEE Trans Dielectr Insulation* 12:914
35. Roy M, Nelson JK, Reed CW (2005) *IEEE Trans Dielectr Insulation* 12:643
36. Panwar V, Sachdev VK, Mehr RM (2007) *Eur Polym J* 43:573